PHYSICAL REVIEW E

STATISTICAL PHYSICS, PLASMAS, FLUIDS, AND RELATED INTERDISCIPLINARY TOPICS

THIRD SERIES, VOLUME 57, NUMBER 3 PART B **MARCH 1998**

ARTICLES

Dynamics of closed interfaces in two-dimensional Laplacian growth

Silvina Ponce Dawson*

Departamento de Física, Facultad de Ciencias Exactas y Naturales, University of Buenos Aires, Ciudad Universitaria, Pabellón I, 1428 Buenos Aires, Argentina

Mark Mineev-Weinstein†

Complex Systems Group, Theoretical Division, Los Alamos National Laboratory, Los Alamos, New Mexico 87545

(Received 13 May 1997)

We study the process of two-dimensional Laplacian growth in the limit of zero-surface tension for cases with a closed interface around a growing bubble (*exterior problem with circular geometry*). Using the time-dependent conformal map technique we obtain a class of fingerlike solutions that are characterized by a finite number of poles. We find the conditions under which these solutions remain smooth for all times. These solutions allow the description of the system in terms of a finite number of degrees of freedom, at least in the limit of zero-surface tension. We believe that, whenever they remain smooth, they can also be used as a nonlinear basis even when surface tension is included. [S1063-651X(98)03102-X]

PACS number(s): 68.10.−m, 47.15.Hg, 47.20.Hw, 68.70.+w

I. INTRODUCTION

The problem of pattern formation is one of the most rapidly developing branches of nonlinear science today (see, e.g., [1]). In particular, the study of the dynamics of fronts between two phases (*interfaces*) has motivated a large body of work in the area [2]. This type of processes occur in a variety of nonequilibrium systems, including physical (viscous fingering [3], electrodeposition [4], crystal growth [5], etc.), chemical (reactions in continuously fed open reactors [6], etc.), and biological ones (growth of bacterial colonies [7], etc.). In many cases the motion of the interface is much slower than the processes that take place in the bulk of the phases (such as heat transfer, diffusion, etc.). In those cases, the scalar field governing the evolution of the interface is a harmonic function and, therefore, it is reasonable to call the whole process *Laplacian growth*. Furthermore, when a two-dimensional description is possible (as, for example, when the relevant quantities can be averaged along one direction) we talk about two-dimensional (2D) Laplacian growth. In this paper we will be concerned with processes that allow this decription.

The physical meaning of the scalar field involved in the description differs from system to system. For example, it is a temperature in the Stefan problem, a concentration in the case of solidification, an electrostatic potential in electrodeposition, a pressure in viscous fingering in Hele-Shaw cells, etc. In real systems surface tension is usually present and it prevents the interface from developing features at very small length scales. Furthermore, surface tension is frequently the factor that determines the asymptotic evolution of the system. In fact, experiments in Hele-Shaw cells showed that the system evolved towards a particular solution, although, in theory, there was a continuous set of possible long-term behaviors [8]. This selection problem remained unsolved for a long time until it was shown that surface tension could provide the necessary selection mechanism [9]. On the other hand, although some solutions in the limit of zero-surface tension were obtained and studied [10,11] most of them developed finite-time singularities via the formation of cusps [12,13] (unless they involved some kind of symmetry that prevented this from happening as in [10]). For this reason, *the study with no surface tension was somehow left aside because it was considered a singular and unrealistic limit.*

In spite of this, in previous work [14,15] we showed that there is a whole class of solutions with zero-surface tension that remain smooth for all times. Furthermore, the solutions

*Electronic address: silvina@df.uba.ar

†Electronic address: mariner@lanl.gov

are very general in the sense that no symmetries are assumed. They reproduce many of the features that are observed in experiments, such as tip splitting, sidebranching, screening, and coarsening, some of which were usually attributed to the effect of surface tension [9]. As we mention in [14,15], the smoothness of the solutions does not imply their stability. In fact, how some zero-surface tension solutions are altered when they are considered as the initial condition to the equations with nonzero-surface tension has been extensively studied in [16]. In any case, we must mention that a wider class of zero-surface tension solutions has been found (which includes the ones studied in [14,15] as a particular case), which is indeed an attractor in the case of channel geometry [17]. Most amazingly, this attracting zero-surface tension solution reproduces the experimental observation of a single finger whose width is half the width of the channel. This remarkable and unexpected result implies that zero-surface tension solutions are more relevant for realistic situations than has usually been thought of. Under certain assumptions, we proved the smoothness of the zero-surface tension solutions for the case in which the interface is open and infinite and in the case of *channel geometry*. In this paper we investigate whether a similar situation holds when the interface is closed. Closed interfaces are relevant in many experimental situations, such as viscous fingering in radial Hele-Shaw cells [18], isotropic solidification, slow electrodeposition, etc. We expect our study to be relevant for these cases.

We study in this paper the class of fingerlike solutions of 2D Laplacian growth in the case of circular geometry. The solutions are similar to those introduced in [10], but with no symmetries. They are described in terms of a finite number of time-dependent variables (logarithmic poles). Therefore they provide a description of the evolution with a finite number of degrees of freedom. It is worth mentioning that solutions with logarithmic singularities appear to be generic both for the radial and for the rectangular channel geometry [24]. This does not appear to be the case for the ''wedge'' (sector) geometry, where fractional type of singularities might be involved [25]. We study under which conditions the logarithmic pole solutions remain smooth for all times and we find sufficient conditions for this to happen. As in the case of channel geometry [14], these solutions reproduce various phenomena observed in experiments [3]. As in nearly integrable systems, in which the soliton solutions of the integrable limit [19] serve to describe the evolution of the nonintegrable case with a finite number of degrees of freedom [20], we expect these fingerlike solutions to serve as a ''nonlinear basis'' even when surface tension is taken into account. As in the soliton case, this decomposition in terms of a finite number of degrees of freedom should be good regardless of whether each individual solution in the ''basis'' is stable or not. Thus the relevance of whether they remain smooth or not goes beyond the limiting case of zero-surface tension.

The organization of the paper is as follows. In Sec. II we introduce the equations with which we model the problem of interest. We show in this section how to obtain the Laplacian growth equation and present the class of exact solutions that we are going to analyze in the paper. In Sec. III we analyze the class of asymptotic behaviors that remain free of singularities. In Sec. IV we analyze which initial conditions can approach the smooth asymptotic behaviors of Sec. III. In Sec. V we introduce a model in order to analyze whether the conditions we find in the asymptotic limit for the solution to be well behaved need to be satisfied before the asymptotic regime is reached. In Sec. V we describe a set of numerical simulations to analyze this in more general cases. Finally, we summarize the results in Sec. VI.

II. THE MATHEMATICAL SETTING

We consider a system in two spatial dimensions, $\mathbf{R}\equiv(X,Y)$, composed of two different phases separated by a closed moving interface, $\Gamma(t)$. Let us call I the region enclosed by Γ and II the region outside. Both regions are simply connected. There is a scalar field, $P(X,Y)$, that describes the state of each phase, for example, pressure. We assume that this field satisfies the Laplace equation in region II, subject to the boundary conditions of it being constant on Γ and that $P\sim-\ln(|\mathbf{R}|)$ as $|\mathbf{R}|\to\infty$. This last condition is suitable for a case in which region I corresponds to a growing bubble and the quantities have been rescaled so that the extraction rate at infinity is equal to -2π [10]. In this way the dynamical problem is described by the following equations:

$$\nabla^2 P=0, \quad \mathbf{R}\in \mathrm{II}, \tag{1}$$

$$P\sim-\ln(|\mathbf{R}|), \quad |\mathbf{R}|\to\infty, \tag{2}$$

$$P|_{\Gamma(t)}=0, \tag{3}$$

$$v_n|_{\Gamma(t)}=-(\nabla P)_n, \tag{4}$$

where $\mathbf{v}$ is the interface velocity and the subscript n represents the component normal to the interface. This set has to be supplemented with initial conditions for the form of the interface.

In order to look for a solution of Eqs. (1)–(4) we identify the physical space with the complex plane and use the conformal mapping technique. Thus, we define the complex coordinate $Z\equiv X+iY\equiv Re^{i\Phi}$, in the *physical plane*, and the complex pressure $W(Z)\equiv P(X,Y)+i\Psi(X,Y)$, where i is the imaginary unit and $\Psi(X,Y)$ is a real function harmonically conjugated to $P(X,Y)$. Then, we introduce a *mathematical plane*, which we also identify with the complex plane, $z\equiv x+iy\equiv re^{i\varphi}$, and define a time-dependent conformal map f, $Z\equiv f(z,t)$, from the region outside the unit circle in the mathematical plane ($|r|>1$), to region II of the physical plane. In this way, the moving interface Γ is the image of the border of the unit circle under the conformal map. In these new coordinates Eqs. (1)–(4) reduce to (see, e.g., [10,15])

$$\frac{\partial W}{\partial \bar{z}}=0, \quad |z|>1 \tag{5}$$

$$\frac{dW}{dz}\to-\frac{1}{z} \quad \text{as } z\to\infty, \tag{6}$$

$$\mathrm{Re}W=0 \quad \text{at } |z|=1, \tag{7}$$

and the Laplacian growth equation (or LGE [14,15]) for $f(z,t)$:

$$\mathrm{Re}\left(z\frac{\partial f}{\partial z}\overline{\frac{\partial f}{\partial t}}\right)=1 \quad \text{at } |r|=1. \tag{8}$$

This equation was originally derived in 1945 [21] and has several remarkable properties. It has an infinite number of constants of motion [22] (see also extensions to multidimensional and multiconnected systems [23]), and it is integrable [24].

Because the map f must be conformal outside the unit circle, it is necessary that all zeros and singularities of $\partial f/\partial z$ be located inside the unit circle. On the other hand, very far away from the interface all quantities will have the same form in both systems of coordinates, z and Z. Therefore we also require that $f(z,t)\approx r(t)z$ for $|r|\to\infty$, where $r(t)$ is the size of the growing domain (unless the domain is fractal). Given these features, we propose a solution whose derivative has the form

$$\frac{\partial f(z,t)}{\partial z}=r(t)\frac{\Pi_{\ell=1}^{N}[z-z_\ell(t)]}{\Pi_{\ell=1}^{N}[z-\zeta_\ell(t)]}, \tag{9}$$

with r, ζ_ℓ, and z_ℓ functions of time t, and $|\zeta_\ell|<1$, $|z_\ell|<1$ for all times and $1\leqslant\ell\leqslant N$. In fact, Eq. (8) has solutions that satisfy Eq. (9) which can be written as

$$f(z,t)=r(t)z-\sum_{\ell=1}^{N}\alpha_\ell(t)\ln\zeta_\ell(t)+\sum_{\ell=1}^{N}\alpha_\ell(t)\ln[z-\zeta_\ell(t)], \tag{10}$$

where

$$\sum_{\ell=1}^{N}\alpha_\ell=0, \tag{11}$$

for f to be single valued, and the equations that $r(t)$ and the various $\zeta_\ell(t)$ satisfy can be obtained inserting Eq. (10) in Eq. (8). In particular, the function $r(t)$ is determined by the area $\mathcal{A}$ enclosed by the curve Γ in the physical plane. In fact, using the conformal map and Eq. (8) it can be easily shown that the area satisfies $d\mathcal{A}/dt=2\pi$. Using then the relation $\mathcal{A}=(1/2i)\oint_{|z|=1}\overline{f}(\partial f/\partial z)dz$ and defining $r_0\equiv r(0)$, we get

$$t=\frac{r^2-r_0^2}{2}+\sum_{\ell,k=1}^{N}\frac{\alpha_\ell\overline{\alpha_k}}{2}\ln\left(\frac{1-\zeta_\ell(t)\overline{\zeta_k(t)}}{1-\zeta_\ell(0)\overline{\zeta_k(0)}}\right). \tag{12}$$

If we substitute Eq. (10) in Eq. (8) we find that all α_ℓ's are time independent and that the dynamics of the poles ζ_ℓ, $\ell=1,N$ is governed by N complex constants of motion β_k which are given by

$$\beta_k=\frac{r(t)}{\overline{\zeta_k(t)}}+\sum_{\ell=1}^{N}\alpha_\ell\ln\left(\frac{1}{\zeta_\ell(t)\overline{\zeta_k(t)}}-1\right) \tag{13}$$

(also see [15]). Using these constants we can rewrite Eq. (12) as

$$t=\frac{r^2-r_0^2}{2}+\frac{r_0}{2}\sum_{k=1}^{N}\frac{\overline{\alpha_k}}{\overline{\zeta_k(0)}}-\frac{r}{2}\sum_{k=1}^{N}\frac{\overline{\alpha_k}}{\overline{\zeta_k(t)}}. \tag{14}$$

In summary, the solution (10) is uniquely determined by the constants α_ℓ and the functions $r(t)$ and $\zeta_\ell(t)$, $1\leqslant\ell\leqslant N$. Hence, the zeros of $\partial f/\partial z$, z_ℓ, $1\leqslant\ell\leqslant N$ are also determined by these quantities and are, therefore, functions of time.

Now, this construction allows us to obtain a solution of the original problem while the poles and zeros of $\partial f(z,t)/\partial z$ remain inside the unit circle. Since they evolve in time it is not clear that, even if they are inside the unit circle at $t=0$, they will remain inside for all times. The aim of this paper is to obtain conditions that guarantee that this happens for all times. This is similar to what we have done for channel geometry [14,15]. Actually, in this case, we will usually consider r as the independent variable and write $\zeta_k(r)$ and $z_k(r)$. It is clear that differentiating Eq. (13) by r we immediately obtain evolution equations for the poles $\zeta_k(r)$ as functions of r. Given r and $\zeta_k(r)$, $1\leqslant k\leqslant N$, we obtain $t(r)$ through Eq. (12) or (14). This way of constructing the solution will work while t is an increasing function of r. Actually it is possible to show that, if there is a value of r ($r=r_0$) at which $dt/dr=0$, then there is at least a zero z_k or a pole ζ_ℓ such that $|z_k(r_0)|=1$ or $\zeta_\ell(r_0)=1$. Thus the invertibility of $t(r)$ is a necessary condition for the zeros to be inside the unit circle. In order to determine the conditions under which the solution remains valid for all times, we analyze first the asymptotic behaviors (as $t\to\infty$) that are compatible with the zeros and poles remaining inside the unit circle. We then study the subclass of initial conditions which can provide these asymptotic behaviors.

III. POSSIBLE ASYMPTOTIC BEHAVIORS

We now look for the possible asymptotic behaviors that are compatible with two constraints of the problem: the constants of motion defined in Eq. (13) and the condition $|\zeta_\ell(t)|<1$ for all times and ℓ's. Since the quantity $r^2(t)$ is mainly determined by the total area enclosed by Γ, we expect it to be an increasing function of time. Therefore we look for asymptotic behaviors for which $r(t)\to\infty$ as $t\to\infty$. Let us write the constants α_ℓ as

$$\alpha_\ell\equiv|\alpha_\ell|e^{i\lambda_\ell}, \quad 1\leqslant\ell\leqslant N \tag{15}$$

and the location of the poles ζ_ℓ as

$$\zeta_\ell(t)\equiv|\zeta_\ell(t)|e^{i\gamma_\ell(t)}, \quad 1\leqslant\ell\leqslant N. \tag{16}$$

We see that an asymptotic behavior that allows the conservation of the quantities in Eq. (13) is

$$r\to\infty, \tag{17}$$

$$|\zeta_\ell|\to 1, \quad 1\leqslant\ell\leqslant N. \tag{18}$$

In this way the divergence of the term proportional to r in the constants β_ℓ can be canceled out by another divergent term, $\alpha_\ell\ln(1/|\zeta_\ell|^2-1)$. In particular, *if all λ_ℓ's are different* we obtain, under certain conditions that we will discuss later and which guarantee that all γ_ℓ's approach different values as $r\to\infty$, the following relations:

$$|\zeta_\ell| \approx 1 - \frac{\delta_\ell}{2} e^{-r/|\alpha_\ell|}, \tag{19}$$

$$\gamma_\ell \approx \lambda_\ell + \frac{\epsilon_\ell}{r} \quad \text{as} \quad t \to \infty, \tag{20}$$

for $1 \leq \ell \leq N$. In Eqs. (19) and (20) δ_ℓ and ϵ_ℓ are real constants that can be obtained from the conserved quantities β_ℓ in the limit of $r \to \infty$, when all $|\zeta_\ell| \to 1$ and all γ_ℓ's approach different values. They are

$$\ln \delta_\ell = \mathrm{Re}\left[\frac{\beta_\ell}{\alpha_\ell} - \sum_{k \neq \ell} \frac{\alpha_k}{\alpha_\ell} \ln(e^{i(\lambda_\ell - \lambda_k)} - 1) \right], \tag{21}$$

$$\epsilon_\ell = \mathrm{Im}\left[\beta_\ell e^{-i\lambda_\ell} - \sum_{k \neq \ell} |\alpha_k| e^{i(\lambda_k - \lambda_\ell)} \ln(e^{i(\lambda_\ell - \lambda_k)} - 1) \right]. \tag{22}$$

We have to look now at how the zeros of $\partial f / \partial z$, $z_k(t)$, evolve when $r(t)$ and the poles behave as in Eqs. (17)–(20). In particular, we do not know if it is necessary to impose some other restrictions on the asymptotic behavior for the zeros to remain inside the unit circle. In order to analyze this, let us define $P(z) \equiv \Pi_{k=1}^{N} (z - z_k)$. Using Eqs. (9) and (10) we can write

$$P(z) = r \prod_{\ell=1}^{N} (z - \zeta_\ell) + \sum_{k=1}^{N} \alpha_k \prod_{\ell \neq k} (z - \zeta_\ell). \tag{23}$$

It is possible to show that $P(z)$ is the characteristic polynomial of the matrix A defined by

$$A_{kj} = \zeta_k \delta_{kj} - \frac{\alpha_k}{r}, \tag{24}$$

where δ_{kj} is the Kronecker symbol. Thus the zeros z_k of $P(z)$ are the eigenvalues of the square matrix A. According to Gerschgorin's theorem (see, e.g., [26]) the eigenvalues of an $N \times N$ square matrix A lie in the union of the N disks Γ_k defined by $\Gamma_k : |z - A_{kk}| \leq \Sigma_{j=1, j \neq k}^{N} |A_{kj}|$. Therefore applying Gerschgorin's theorem to our matrix A we find that its eigenvalues, or equivalently, the zeros z_k of $\partial f / \partial z$ satisfy

$$\left| z_k - \zeta_k + \frac{\alpha_k}{r} \right| \leq \frac{1}{r} \min\left\{ \sum_{\ell \neq k}^{N} |\alpha_\ell|, (N-1)|\alpha_k| \right\}$$

$$\text{for all} \quad 1 \leq k \leq N. \tag{25}$$

Thus, using Eqs. (17)–(20) we find that

$$z_k \to e^{i\lambda_k} \qquad \text{as} \quad r \to \infty. \tag{26}$$

Furthermore, we get from Eq. (23) the following relation:

$$\frac{\alpha_k}{r} = (\zeta_k - z_k) \prod_{\ell \neq k} \left(\frac{\zeta_k - z_\ell}{\zeta_k - \zeta_\ell} \right) = (\zeta_k - z_k) \prod_{\ell \neq k} \left(1 + \frac{\zeta_\ell - z_\ell}{\zeta_k - \zeta_\ell} \right), \tag{27}$$

provided that all ζ_k's are different. This holds, in particular, when the asymptotic behavior is described by Eqs. (19) and (20) and all the arguments, λ_ℓ, are different. We see from

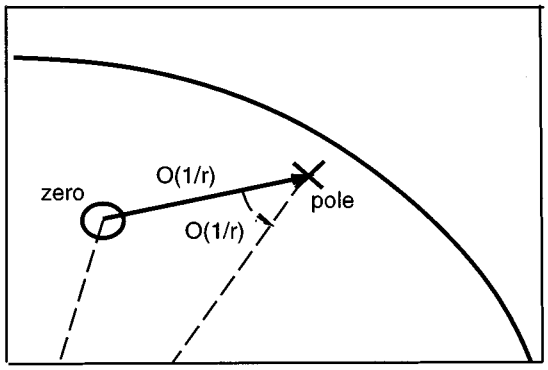

FIG. 1. Schematic picture of how poles and zeros can be distributed in the mathematical plane in the asymptotic limit described by Eqs. (19)–(22). The solid line indicates (part of) the border of the unit circle. The cross indicates the location of a pole ζ_1 and the small circle that of a zero z_1 for r big enough. The difference between both is $\zeta_1 - z_1 = \alpha_1 / r$, which is also shown in the figure as the arrow of length of $O(1/r)$. The distance from ζ_1 to the border is $O(e^{-|\alpha_1|/r})$. Given that the arguments of ζ_1 and α_1 are almost equal [they differ by a quantity of $O(1/r)$ as indicated in the figure] z_1 lies inside the unit circle and further away from the border than ζ_1, its distance being $O(-|\alpha_1|/r)$.

Eq. (27) that its right hand side goes to zero as $r \to \infty$. We then conclude that $(\zeta_k - z_k) \to 0$ as $r \to \infty$. Moreover, assuming that α_k / r is small enough for each k we get from Eq. (27) the relation

$$z_k = \zeta_k - \frac{\alpha_k}{r} + \frac{1}{r^2} \sum_{\ell \neq k} \frac{\alpha_k \alpha_\ell}{(\zeta_k - \zeta_\ell)} + O\left(\left[\frac{|\alpha|}{r} \right]^3 \right). \tag{28}$$

Combining Eqs. (28) and (19) and (20) we obtain

$$z_k \approx e^{i\lambda_k} \left(1 - \frac{|\alpha_k|}{r} + i \frac{\epsilon_k}{r} \right) \quad \text{as} \quad r \to \infty. \tag{29}$$

Thus $|z_k|^2 \approx 1 - 2|\alpha_k|/r < 1$ for r big enough.

Hence, we find that, for r big enough, it is possible to have a solution of the form (10) such that all zeros and poles of $\partial f / \partial z$ lie inside the unit circle. Such a solution has the property that the argument of each pole ζ_k and each zero z_k differ from the argument of the corresponding constant α_k by a very small amount, which is of the order of $1/r$ with r big. The fact that $\cos(\gamma_k - \lambda_k) > 0$ for r big guarantees, on one hand, that the sum of the two divergent terms in the constants β_k goes to a finite limit as $r \to \infty$. On the other hand, it guarantees that the zeros remain ''behind'' the poles and cannot reach the unit circle at a finite value of r. We show a schematic picture of this behavior in Fig. 1. In the next two sections we analyze whether the alignment of the singularities and the α's (i.e., $\lambda_k \approx \gamma_k$ for all k) needs to be satisfied also for small values of r, in order for an initial condition to be able to reach the smooth asymptotics just described.

This asymptotic regime shares some properties with the one we found in the channel and in the infinite line geometries [14,15], i.e., a case in which the interface is not closed. In that case we used a conformal map that mapped the real axis of the mathematical plane onto the physical interface, but still it is possible to make some connections with the case

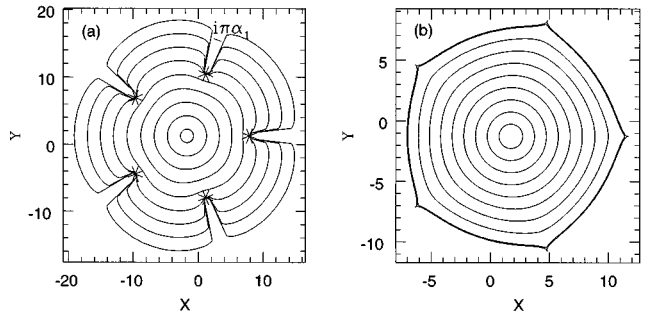

FIG. 2. (a) Physical interface at different times for a solution of the form (10) with $N=5$, $\{\alpha_k\}_{k=1}^{N}$ as in Eq. (35) with $\Lambda=0.4$, and $\{\zeta_k(r_0)\}_{k=1}^{N}$ as in Eq. (36) with $|\zeta_k(r_0)|=0.1$ and $r_0=1$. The location of the stagnation points is indicated with asterisks. A straight line of length $\pi\alpha_1$ along the vector $i\alpha_1$ has been drawn inside the corresponding ''gap'' of the interface. (b) Similar to (a) but here $\gamma_k(r_0)=\lambda_k(r_0)+\pi$ for all $1\leqslant k\leqslant 5$. In this case the solution develops cusps at a finite time.

we are analyzing now. In particular, it is possible to show in the present case that, as $r\to\infty$, the interface develops ''stagnation points,'' i.e., points that stay almost fixed during the evolution. Let us remember that the physical interface is given by the curve $f(z=e^{i\varphi})$ with $-\pi\leqslant\varphi\leqslant\pi$. Using the formulas that describe the asymptotic regime, Eqs. (19)–(22), and Eq. (13) we find

$$f(z=e^{i\gamma_k})=\beta_k-\alpha_k\ln 2+O\left(\frac{|\alpha|}{r}\right), \tag{30}$$

where care should be taken in order to choose the argument of the logarithms. In any case, this shows that there are as many stagnation points as poles and that their location is determined by the constants of motion of the problem. On the other hand, if we consider a range of angles φ in a small neighborhood of γ_k we find

$$f(e^{i\varphi})=\beta_k-\alpha_k\ln 2+i\alpha_k\arctan\left[\frac{\varphi-\gamma_k}{1-|\zeta_k|}\right]+O\left(\frac{|\alpha|}{r}\right). \tag{31}$$

Since $1-|\zeta_k|\to 0$ as $r\to\infty$, the argument of the arctan in Eq. (31) can be very big even if $\varphi-\gamma_k$ is very small. In fact, we can always find $\Delta=\eta(1-|\zeta_k|)$ such that $\eta\gg 1$ but $\Delta\ll 1$. In this way we can consider the range of angles $\varphi_{\min}\equiv\gamma_k-\Delta\leqslant\varphi\leqslant\varphi_{\max}\equiv\gamma_k+\Delta$ for which Eq. (31) is valid. On the other hand, since $\eta\gg 1$, then

$$-\arctan\left[\frac{\varphi_{\min}-\gamma_k}{1-|\zeta_k|}\right]=\arctan\left[\frac{\varphi_{\max}-\gamma_k}{1-|\zeta_k|}\right]=\arctan\left[\frac{\Delta}{1-|\zeta_k|}\right]$$
$$=\arctan[\eta]\approx\frac{\pi}{2}. \tag{32}$$

Thus we obtain from Eq. (31) the relation

$$f(e^{i\varphi_{\max}})-f(e^{i\varphi_{\min}})=i\pi\alpha_k. \tag{33}$$

This implies that the interface has ''gaps'' around each stagnation point of width $\pi|\alpha_k|$ with an orientation that depends exclusively on each α_k. We call a finger the region between two gaps. We illustrate this in Fig. 2(a) where we have plotted the physical interface for a solution of the form (10) with $N=5$, that remains smooth for all times. There we indicate the location of the stagnation points with crosses. We have also drawn a straight line of length $\pi\alpha_1$ along the vector $i\alpha_1$ inside the corresponding ''gap'' of the interface. We observe a total of five gaps and five fingers, i.e., as many as poles.

In the case of channel geometry we also found solutions such that two gaps corresponding to two different poles merged into one gap. We related this to the effect of shielding observed in experiments of viscous fingering, since the finger between the two gaps of the analytical solution stopped growing after some time. In fact, we can also find this type of solutions in the present case. However, the asymptotic behavior is not described by Eqs. (19)–(22). In this case two arguments, for example, γ_1 and γ_2, approach the same number as $r\to\infty$. This number is neither λ_1 nor λ_2, but lies in between the two. In this case, there are more than two diverging terms in β_1 and β_2, as $r\to\infty$, and one needs to take all of them into account in order to deduce asymptotic expressions for the poles ζ_1 and ζ_2. The asymptotic value of γ_1 and γ_2 is $\arg(\alpha_1+\alpha_2)$. Two initially separated gaps described by $\{\alpha_1,\beta_1\}$ and $\{\alpha_2,\beta_2\}$ will eventually merge if

$$\cos(\theta_1)>\cos(\theta_2),$$
$$\sin(\theta_1)\sin(\theta_2)\geqslant 0, \tag{34}$$

where $\theta_{1,2}=\lambda_{1,2}-\arg(\beta_1/\beta_2)$.

It should also be possible to find smooth asymptotic behaviors in cases for which some arguments, λ_k, are equal. We are not going to analyze these cases in the present paper. Thus we will assume from now on that $\lambda_k\neq\lambda_j$ for all $k\neq j$.

IV. ABOUT INITIAL CONDITIONS LEADING TO NONSINGULAR ASYMPTOTIC BEHAVIORS

Now that we have obtained a set of smooth asymptotic behaviors, which are defined by Eqs. (17)–(20), we look for sets of initial conditions with finite values of r that can reach such asymptotics. A ''good'' initial condition must be such that $|\zeta_k(0)|<1$ and $|z_k(0)|<1$ for all $1\leqslant k\leqslant N$. It is easy to construct such an initial condition. Given the number of singularities, N, we first choose a set of N complex numbers α_k constrained by Eq. (11). We then choose $r(0)$ so that $N\Lambda/r(0)<1$, where $\Lambda\equiv\max_k\{|\alpha_k|\}$. Then, we choose a set of real numbers $|\zeta_k(0)|$ sufficiently small so that all the balls defined in Eq. (25) are entirely contained in the unit circle. We can always do this provided that $N\Lambda/r(0)<1$. In this way we guarantee that all zeros satisfy $|z_k(0)|<1$. Now, even if we construct such an initial condition we cannot guarantee that the solution will be well behaved for all times: either a pole or a zero might cross the unit circle at a finite time. Almost all known solutions of Eq. (8) develop finite-time singularities via the formation of cusps and this has been the subject of a large amount of work during the past years. Despite these negative results, we were able to obtain, in a different geometry, a class of solutions that remained smooth for all times [14,15]. Although we do not have a proof in the present case, we have obtained a set of addi-

tional constraints that seem to guarantee the smoothness of the solution at all times.

As we mentioned in the preceding section, in the smooth asymptotics each pole ζ_k is almost aligned with its corresponding α_k. Thus we ask whether it is necessary that the initial condition have this property too, in order to be able to reach the good asymptotics. In particular, it has been shown that certain solutions of the form (10) that have some type of symmetries do remain smooth for all times [10]. These symmetric solutions have the ''alignment'' property during the whole evolution. A particular subset of this class is the one for which

$$\alpha_k=\Lambda e^{\frac{2\pi i k}{N}}, \quad \Lambda \ \text{ real}, \quad k=1,\ldots,N \tag{35}$$

and the initial condition is such that

$$|\zeta_k(t=0)|<1, \quad \gamma_k(t=0)=\frac{2\pi k}{N}, \quad k=1,\ldots,N. \tag{36}$$

It is possible to show that the poles are of the form

$$\zeta_k(t)=\psi(t)e^{2\pi i k/N}, \quad \psi(t) \ \text{ real}, \tag{37}$$

for all $t\geqslant 0$, so that $\gamma_k(t)=\lambda_k$ for all times. We show in Fig. 2(a) various snapshots of the physical interface for one such symmetric solution with $N=5$, where we see that it does remain smooth during the whole evolution. If we take an initial condition as the one described by Eqs. (35) and (36) but with $\gamma_k(0)=\lambda_k+\pi$ instead of $\gamma_k(0)=\lambda_k$, the arguments γ_k also remain constant during the evolution. Thus they cannot reach the asymptotic regime described by Eqs. (19)–(22), since the arguments of the poles will never align with those of the α_k's. Notice that by choosing this initial condition we interchange the mutual position of zeros and poles with respect to the previous case. In this way, the zeros reach the unit circle at a finite time and the solution develops cusps (this case was studied in [13]). We show a plot of the physical interface in Fig. 2(b) for one such solution.

Now, the discussion of the preceding section shows that there can be nonsymmetric solutions that give rise to smooth interfaces, at least in the asymptotic regime. In order to determine how important the alignment property is from the very beginning, we analyze first a model, which we describe in the next section, and then perform a series of numerical simulations that cover a wide range of situations.

V. SIMPLIFIED MODEL: IS THE ALIGNMENT NECESSARY FROM THE VERY BEGINNING?

In order to analyze whether the alignment is necessary from the very beginning, we introduce here a model that applies in certain cases. Let us first define the following quantities:

$$\hat{\beta}_k=\frac{r(t)}{\overline{\zeta_k(t)}}+\sum_{\ell=1}^{N}\alpha_\ell \ln[1-\zeta_\ell(t)\overline{\zeta_k(t)}]. \tag{38}$$

Using the fact that $\Sigma_{k=1}^{N}\alpha_k=0$, it is possible to show that the quantities $\hat{\beta}_k$ are related to the constants of motion, β_k, defined in Eq. (13), by

$$\hat{\beta}_k=\beta_k-\sum_{\ell=1}^{N}\alpha_\ell \ln(\zeta_\ell). \tag{39}$$

Let us assume now that the norms of the poles are initially very small [$|\zeta_k(r_0)|\ll 1$ for all k]. In such a case we can approximate the quantities $\hat{\beta}_k$ by

$$\hat{\beta}_k\approx\frac{r}{\overline{\zeta_k(r)}}, \tag{40}$$

while $|\alpha_\ell\zeta_k(r)\zeta_\ell(r)|\ll r/|\zeta_k(r)|$ for all ℓ and k and $|r/r_0-1|\ll 1$. If we replace Eq. (39) in Eq. (40) and differentiate the resulting equation with respect to r we observe that, for $|\zeta_k|$ small enough, the variation of $\Sigma_{\ell=1}^{N}\alpha_\ell\ln(\zeta_\ell)$ with r is much smaller (in norm) than that of $r/\overline{\zeta_k(r)}$. This in turn implies that $d\ln\zeta_\ell/dr=1/r$ for all ℓ. Therefore, in this approximation, $d/dr[\Sigma_{\ell=1}^{N}\alpha_\ell\ln(\zeta_\ell)]=0$, implying that the quantities $\hat{\beta}_k$ can be treated as constants.

Let us consider now the pole with the largest norm and let us assume that it remains the one with the largest norm during the whole evolution. Without loss of generality we can say it is the one with $k=1$. Given that all λ_k's are different, neglecting all terms with $\ell\neq 1$ in Eq. (38), we get the following approximate relations:

$$\hat{\beta}_1 e^{-i\lambda_1}\approx\frac{re^{i[\gamma_1(r)-\lambda_1]}}{|\zeta_1(r)|}+|\alpha_1|\ln[1-|\zeta_1(r)|^2], \tag{41}$$

which reduces to Eq. (40) if $|\zeta_1|$ is small enough, and

$$t\approx\frac{r^2-r_0^2}{2}+\frac{|\alpha_1|^2}{2}\ln[1-|\zeta_1(r)|^2]. \tag{42}$$

Given that, at least initially, $|\zeta_1|\approx r/|\hat{\beta}_1|$ [see Eq. (40)], we conclude from Eq. (42) that $|\hat{\beta}_1/\alpha_1|>1$ for time t to increase monotonically with r. Therefore we assume that $|\hat{\beta}_1/\alpha_1|>1$. We also assume that the approximate relations (40) are still valid for all $k\neq 1$. From Eq. (40) it immediately follows that all $\hat{\beta}_k$ with $k\neq 1$ can be treated as constants. On the other hand, since the departure from the approximate relation (40) for $k=1$ occurs when r becomes sufficiently large so that $|\zeta_1|$ is close to one, we can show that $\hat{\beta}_1$ can also be treated as a constant. In fact, in all the simulations we show in this paper the various $\hat{\beta}_k$'s remain practically constant. Moreover, if we integrate the equations for the poles assuming that either the $\hat{\beta}_k$'s or the β_k's are constant, we get evolutions which are almost indistinguishable. Notice then that Eq. (41) not only reduces to Eq. (40) if $|\zeta_1|$ is small, but it also ''contains'' the asymptotic behavior described by Eqs. (19) and (20) as $r\to\infty$.

Assuming the approximation is good, we get from Eq. (41)

$$\frac{r^2}{|\alpha_1|^2}=|\zeta_1(r)|^2\left[\left(a+\ln\frac{1}{1-|\zeta_1(r)|^2}\right)^2+b^2\right], \quad (43)$$

where $a=\mathrm{Re}(\hat{\beta}_1/\alpha_1)$ and $b=\mathrm{Im}(\hat{\beta}_1/\alpha_1)$. Inserting Eq. (43) in Eq. (42) we obtain

$$\tau\equiv\frac{2t+r_0}{|\alpha_1|^2}=x\left[\left(a+\ln\frac{1}{1-x}\right)^2+b^2\right]-\ln\frac{1}{1-x}, \quad (44)$$

where $x=|\zeta_1(r)|^2$. As mentioned before, if $|\hat{\beta}_1/\alpha_1|>1$, both x and τ are, initially, increasing functions of r. Thus, at the initial stages, τ is an increasing funcion of x. If this continues to be so for all $0\leqslant x<1$, then the behavior is smooth, i.e., there are no finite-time singularities. Note that this monotonic behavior of $\tau(x)$ guarantees, through Eq. (42), that r is also an increasing function of x. This corresponds to the actual behavior of the physical system: the area covered by the ''bubble'' grows with time. On the other hand, if $d\tau/dx=0$ at some value of x, $0<x<1$, then time would need to flow backwards at that point in order to reach the asymptotic behavior as $x\to 1$. This is clearly unphysical and corresponds to the formation of a cusp in the interface at that finite time.

The criterion for the monotonicity of $\tau(x)$ can be found very simply. We want to know if there is an $x_0\in[0,1)$ such that $\tau'(x_0)\equiv d\tau/dx(x_0)=0$. The function $\tau'(x)$ reads

$$\tau'(x)=\left(a+\ln\frac{1}{1-x}\right)^2+b^2+2\frac{x}{1-x}\left(a+\ln\frac{1}{1-x}\right)-\frac{1}{1-x}, \quad (45)$$

and can be rewritten as

$$\tau'=(a^2+b^2)+2a(y+e^y-1)+y^2+2y(e^y-1)-e^y, \quad (46)$$

with $y\equiv-\ln(1-x)$, so $y\geqslant 0$. Because of the smallness of $|\zeta_1(r_0)|$, we obtain from Eq. (41) that $a\approx|\hat{\beta}_1/\alpha_1|\cos[\gamma_1(r_0)-\lambda_1]$. Therefore the sign of a is related to the initial alignment between the pole ζ_1 and α_1. In this way $a>0$ means that $|\gamma_1(r_0)-\lambda_1|<\pi/2$ and vice versa.

Let us define $h(y)\equiv y^2+2y(e^y-1)-e^y$ and $g(y)\equiv(y+e^y-1)$. It is clear that $g(y)\geqslant 0$, for $y\geqslant 0$. On the other hand, $h(y)\geqslant h_{\min}\approx-1.094$, for $y\geqslant 0$. Using the equations $a^2+b^2=|\hat{\beta}_1/\alpha_1|^2$ and $a=|\hat{\beta}_1/\alpha_1|\cos[\gamma_1(r_0)-\lambda_1]$, we obtain from Eq. (46) that a finite-time singularity occurs if there is a $y\geqslant 0$ such that $\tau'(y)=0$. We then conclude that, if $|\hat{\beta}_1/\alpha_1|^2>1.1$ and $|\gamma_1(r_0)-\lambda_1|<\pi/2$, there are no finite-time singularities. Notice that, if $|\zeta_1|\ll r_0$, while $r_0\geqslant|\alpha_1|$, then $|\hat{\beta}_1/\alpha_1|\gg 1$, so that the condition $|\hat{\beta}_1/\alpha_1|^2>1.1$ is automatically satisfied.

We analyze now what happens when $a<0$. Let us assume again that $a^2+b^2=|\hat{\beta}_1/\alpha_1|^2>-h_{\min}$. Using the equations $a^2+b^2=|\hat{\beta}_1/\alpha_1|^2$ and $a=|\hat{\beta}_1/\alpha_1|\cos[\gamma_1(r_0)-\lambda_1]$, we obtain from Eq. (46) that a finite-time singularity will occur if there is a $y\geqslant-\ln 2$ such that

$$\cos[\gamma_1(r_0)-\lambda_1]=k(y)\equiv-\frac{|\hat{\beta}_1/\alpha_1|^2+h(y)}{2g(y)|\hat{\beta}_1/\alpha_1|}. \quad (47)$$

Note that if, as mentioned before, $|\hat{\beta}_1/\alpha_1|\gg 1$, then the condition that $|\hat{\beta}_1/\alpha_1|^2+h(y)>0$ is automatically satisfied. Therefore $k(y)<0$, for $y>0$. So, finite-time singularities never occur if $\cos[\gamma_1(r_0)-\lambda_1]>0$, which corresponds to the case in which the singularity and α_1 are somehow ''aligned.'' On the other hand, $k(y)$ has only one maximum, k^*, such that

$$k^*\equiv k(y_{\max})=-\frac{2\ln(|\hat{\beta}_1/\alpha_1|)+O(1)}{|\hat{\beta}_1/\alpha_1|}. \quad (48)$$

Taking this into account the criterion for a cusp formation is

$$\mathrm{Re}(|\hat{\beta}_1/\alpha_1|)+2\ln(|\hat{\beta}_1/\alpha_1|)<0. \quad (49)$$

This means that $|\gamma_1(r_0)-\lambda_1|$ has to be bounded away from $\pi/2$ for cusps to occur. This is somehow intuitive: in the asymptotic regime $\gamma_1(r)-\lambda_1\to 0$; thus this asymptotic behavior will never be reached if $|\gamma_1(r_0)-\lambda_1|$ is too far away from zero. On the other hand, for $|\hat{\beta}_1/\alpha_1|$ big enough, k^* increases with $|\hat{\beta}_1/\alpha_1|$ [see Eq. (49)]. Thus the bigger $|\hat{\beta}_1/\alpha_1|$ is, the closer to $\pi/2$ the difference $|\gamma_1(r_0)-\lambda_1|$ needs to be to avoid the singularity. This is also intuitive, since $|\alpha_1|$ is the characteristic time with which $|\zeta_1|$ approaches the value 1 as $r\to\infty$ [see Eq. (19)]. If this time is too short and $|\gamma_1(r_0)-\lambda_1|>\pi/2$, there is no time left for the angle γ_1 to approach the asymptotic value λ_1, and the asymptotic behavior cannot be reached.

In summary, we have obtained that, for cases with $|\hat{\beta}_1/\alpha_1|>-h_{\min}\approx 1.094$, an initial condition will be free of finite-time singularities if and only if

$$|\gamma_1(r_0)-\lambda_1|\leqslant\pi/2, \quad (50)$$

or

$$\pi/2<|\gamma_1(r_0)-\lambda_1|<\arccos[\ln(|\hat{\beta}_1/\alpha_1|)/(|\hat{\beta}_1/\alpha_1|)]. \quad (51)$$

This means that the misalignment between $\zeta_1(r_0)$ and α_1 cannot be bigger than an upper bound, which is very close to $\pi/2$ if $|\hat{\beta}_1/\alpha_1|\gg 1$. We must remember that these conditions have been obtained within the framework of our simplified model, so that they will hold provided that the model is a good approximation of the problem.

VI. NUMERICAL SIMULATIONS

In this section we present a set of numerical simulations with which we try to analyze what type of initial conditions can reach the nonsymmetric asymptotic regime described by Eqs. (19)–(22) in a more general setting. In particular, we wanted to check to what extent the conditions derived in the preceding section could be applied to more general cases. For this purpose, we integrated numerically the evolution equations of the poles for various nonsymmetric initial conditions. We show various snapshots of the physical interfaces in Fig. 3.

Figure 3(a) corresponds to a nonsymmetric case with five poles and initial arguments that satisfy $\cos[\gamma_\ell(r_0)-\lambda_\ell]>0$ for all $1\leqslant\ell\leqslant 5$. Thus, taking into account the previous dis-

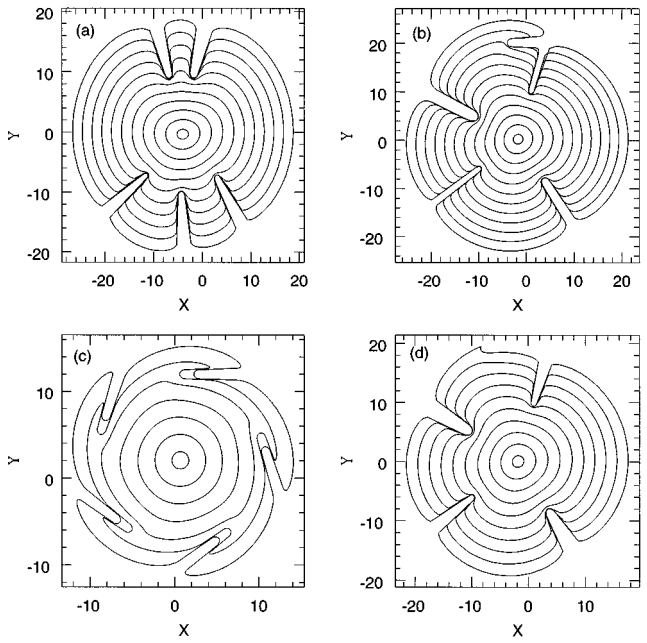

FIG. 3. Physical interfaces at different times for various solutions of the form (10) with different values of N and initial conditions. (a) $N=5$, $|\alpha_1|=0.4$, $|\alpha_2|=0.6$, $|\alpha_3|=0.5$, $|\alpha_4|=0.7$, $\lambda_1=-2.5$, $\lambda_2=-1.5$, $\lambda_3=-1$, $\lambda_4=1.3$, $\alpha_5=-\Sigma_{\ell=1}^{4}\alpha_\ell$; $|\zeta_\ell(r_0)|=0.1$, for $1\leqslant\ell\leqslant5$, $\gamma_1(r_0)=\lambda_1+0.1$, $\gamma_2(r_0)=\lambda_2-0.1$, $\gamma_3(r_0)=\lambda_3+0.2$, $\gamma_4(r_0)=\lambda_4+0.05$, $\gamma_5(r_0)=\lambda_5+0.05$, and $r_0=1$. In this case all $\hat{\beta}_k$'s satisfy $\mathrm{Re}[\hat{\beta}_k(r_0)\exp-i\lambda_k]>0$ and we obtain an asymmetric solution that remains smooth for all times. (b) $N=5$, $|\alpha_1|=0.4$, $|\alpha_2|=0.6$, $|\alpha_3|=0.4$, $|\alpha_4|=0.6$, $\lambda_1=-2.5$, $\lambda_2=-1$, $\lambda_3=1.3$, $\lambda_4=0$, $\alpha_5=-\Sigma_{\ell=1}^{4}\alpha_\ell$; $|\zeta_4(r_0)|=0.05$ and $|\zeta_\ell(r_0)|=0.1$, for all $\ell\neq4$, $\gamma_1(r_0)=\lambda_1$, $\gamma_2(r_0)=\lambda_2$, $\gamma_3(r_0)=\lambda_3$, $\gamma_4(r_0)=\lambda_4+1.6708$, $\gamma_5(r_0)=\lambda_5$, and $r_0=1$. (c) $N=5$ with all α_ℓ's and $|\zeta_\ell(r_0)|$'s as in Fig. 2 but with $\gamma_\ell(r_0)=\lambda_\ell+1.6708$ for all $1\leqslant\ell\leqslant5$. (d) $N=5$, $|\alpha_1|=0.4$, $|\alpha_2|=0.6$, $|\alpha_3|=0.4$, $|\alpha_4|=0.5$, $\lambda_1=-2.5$, $\lambda_2=-1$, $\lambda_3=1.3$, $\lambda_4=0$, $\alpha_5=-\Sigma_{\ell=1}^{4}\alpha_\ell$; $|\zeta_4(r_0)|=0.05$ and $|\zeta_\ell(r_0)|=0.1$, for all $\ell\neq4$, $\gamma_1(r_0)=\lambda_1$, $\gamma_2(r_0)=\lambda_2$, $\gamma_3(r_0)=\lambda_3$, $\gamma_4(r_0)=\lambda_4+1.8708$, $\gamma_5(r_0)=\lambda_5$, and $r_0=1$.

cussion, we expect this initial condition to lead to smooth interfaces for all times. In fact, this is what we observe in the numerical simulation, as shown in Fig. 3(a), where we see smooth nonsymmetric interfaces. In this case the asymptotic behavior is well described by Eqs. (19)–(22), as also illustrated by Fig. 4(a), where we observe how three of the arguments approach the corresponding λ_ℓ's (indicated with dashed lines) while $|\zeta|\to1$.

Figure 3(b) also corresponds to a situation with five poles, but in this case the argument of one of them, ζ_4, satisfies $\cos(\gamma_4-\lambda_4)<0$. The parameters are such that the condition (51) is satisfied [$\cos(\gamma_4-\lambda_4)>-0.1$ and $h(y_{\max})<-0.2$]. Also in this case we observe that the interface remains smooth for all times. Now, this is an example in which the asymptotic behavior is not described by Eqs. (19)–(22), since the arguments of two of the poles, ζ_3 and ζ_4, approach the same value, as shown in Fig. 4(b). The merging of the two arguments results in the merging of the two corresponding gaps, as we can see in Fig. 3(b). It is relatively easy to understand why this happens in terms of the initial condition. In this case $\lambda_3>\lambda_4$ while $\gamma_3(r_0)<\gamma_4(r_0)$. If we assume that

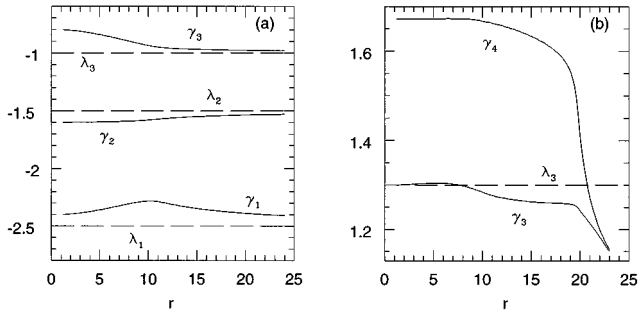

FIG. 4. (a) Plots of γ_1, γ_2, and γ_3 as functions of r for the example of Fig. 3(a). The values of λ_1, λ_2 and λ_3 are indicated with dashed lines. In this case we observe that, for all ℓ, $\gamma_\ell\to\lambda_\ell$ as $r\to\infty$. (b) Plots of γ_3 and γ_4 as functions of r for the example of Fig. 3 (b). In this case γ_3 and γ_4 approach the same value, asymptotically in time, which is neither λ_3 (indicated with a dashed line) nor λ_4 (which is equal to zero) but a value in between.

the asymptotic behavior is described by Eqs. (19)–(22) and that the gaps are aligned as described by Eqs. (31)–(33) we come to the conclusion that the gaps corresponding to these two poles will cross each other. This cannot happen. Instead of this, the two gaps merge and the two arguments approach the same value which is neither λ_3 nor λ_4, as may be observed in Fig. 4(b).

In order to study the validity of the condition (51) without having merging arguments, we tried an initial condition with $N=5$ poles for which $\lambda_1<\lambda_2<\lambda_3<\lambda_4<\lambda_5$, $\gamma_1(r_0)<\gamma_2(r_0)<\gamma_3(r_0)<\gamma_4(r_0)<\gamma_5(r_0)$, and $\cos[\gamma_\ell(r_0)-\lambda_\ell]<0$ for all $1\leqslant\ell\leqslant5$. The results are shown in Fig. 3(c). In this case the condition (51) is satisfied for all the poles ($\cos[\gamma_\ell(r_0)-\lambda_\ell]\approx-0.1$ and $h(y_{\max})\approx-0.247$) and we observe smooth interfaces for all times.

We show in Fig. 3(d) an example in which a cusp develops. The initial condition is similar to that of Fig. 3(b), but in this case ζ_4 does not satisfy the condition (51) [$\cos(\gamma_4-\lambda_4)\approx-0.296$ and $h(y_{\max})\approx-0.178$]. Therefore the evolution agrees with what we expect from this condition.

In summary, the examples we show in Fig. 3 are such that the interfaces remain smooth if the poles either satisfy $\cos(\gamma_\ell-\lambda_\ell)>0$ or $\cos(\gamma_\ell-\lambda_\ell)<0$ and condition (51). On the other hand, if there is at least one pole such that $\cos(\gamma_\ell-\lambda_\ell)<0$ and condition (51) is not satisfied, then the interface develops a cusp. Furthermore, we have observed the same type of behavior for all the initial conditions we tried, regardless of the number of poles. This suggests that the conditions found in the preceding section might apply even if the model is not a very good approximation.

VII. CONCLUSIONS

We have studied the process of two-dimensional Laplacian growth in the limit of zero-surface tension for cases with a closed interface surrounding a growing bubble. We have used the time-dependent conformal map technique to obtain a class of fingerlike solutions. These solutions are similar to those previously found in a different geometry (infinite or periodic, but not closed, interface) [14,15]. They are characterized by a finite number of poles and they are a nonsymmetric generalization of the solutions presented in Ref. [10],

which were limited to specific symmetries.

The study of Laplacian growth is relevant for a variety of physical processes observed both in laboratory experiments and in natural systems, a particular example of which is viscous fingering. Now, the assumption of zero-surface tension is a major limitation of the model. In fact, most solutions studied in the past (see, e.g., [12]) were observed to develop finite-time singularities. As a rule, such singularities would not appear in the presence of surface tension, since its main effect is to prevent the development of small length-scale instabilities. Therefore, in those cases, the zero-surface tension solution is meaningless and does not provide a good representation of the actual evolution. In this paper we have studied under which conditions the nonsymmetric fingerlike solution described by Eq. (10) remains smooth for all times. Using a simplified model we have found some sufficient conditions that guarantee this behavior and others under which the interface becomes singular at a finite time. Apparently these sufficient conditions are also meaningful in cases for which the simplified model assumptions do not hold. In fact, we have observed this in numerical integrations of the solution (10). We have found that whenever each pole satisfies a sufficient condition for the interface to remain smooth, the solution does not become singular. On the other hand, if there is one pole that satisfies the sufficient condition for the development of cusps, then a cusp indeed occurs. Similarly to what happens in the infinite line or channel geometry cases [14], solutions that remain smooth for all times can reproduce various phenomena observed in experiments, such as tip splitting, coarsening, and screening [3]. Therefore they provide a good model of the observed evolution.

One of the interesting properties of these solutions is the fact that they are described in terms of a finite number of time-dependent variables (the poles ζ_k, $1 \leqslant k \leqslant N$). Therefore the evolution is determined by a finite set of ordinary differential equations (ODE's) instead of the original partial differential equation (PDE) (8). The description of infinite-dimensional dynamical systems in terms of finite numbers of degrees of freedom is currently a field of active research. The numerous papers on the theory of inertial manifolds or the technique of proper orthogonal decomposition, among others, are a reflection of this (see, e.g., [27]). The widespread interest in the subject is driven by the possibility of applying well-known results of low-dimensional dynamical systems to infinite-dimensional ones. The existence of a particular class of solutions that allows the reduction of the system, while keeping the main properties of its evolution, provides a unique opportunity of achieving this goal in the present case. Moreover, as in the infinite line and channel geometry cases [14], the reduced system of equations is completely integrable, providing an easy description of the evolution. In this regard, the N-finger solution (10) is similar to the N-soliton solutions of integrable nonlinear partial differential equations.

As in the infinite line and channel geometry cases [14], any smooth initial interface can be approximated, to any degree of accuracy, by an expression of the form (10). Thus, the class of solutions described by Eq. (10) is, in some sense, a nonlinear basis into which any solution of the LGE could be spanned. Now, the choice of N and the various α_k's and $\zeta_k(0)$'s is not unique. We expect that a model with nonzero-surface tension should overcome this selection problem. This does not imply that our zero-surface tension solutions are useless. Consider, for example, the case of slightly perturbed integrable nonlinear PDE's: the soliton solutions of the integrable equations can be used to reduce the analysis of the perturbed ones to a set of ODE's. In some sense, the soliton solutions still form a ''good nonlinear basis'' to study the nonintegrable evolution. We expect a similar situation to hold in our case. Furthermore, the effects of noise on the process of flame propagation have recently been studied in terms of the dynamics of a finite number of poles [28]. This was possible because the model equations had a particular solution that could be written in terms of a finite number of poles. We think a similar analysis could also be done in our case. For these reasons we believe that the solutions we have found are meaningful even when surface tension is included. Thus determining when they remain smooth for all times is relevant in this more general setting.

ACKNOWLEDGMENTS

This work was supported by the University of Buenos Aires, CONICET, and Fundación Antorchas of Argentina and by the U.S. Department of Energy at Los Alamos National Laboratory. Part of this work was done during a visit by S.P.D. at LANL, which she would like to thank for its hospitality and support.

[1] M.C. Cross and P.C. Hohenberg, Rev. Mod. Phys. **65**, 851 (1993).

[2] *Dynamics of Curved Fronts*, edited by P. Pelcé (Academic Press, Inc., Boston, 1988); T. Vicsek, *Fractal Growth Phenomena* (World Scientific, Singapore, 1992).

[3] G.M. Homsy, Annu. Rev. Fluid Mech. **19**, 271 (1987).

[4] M. Matsushita, M. Sano, Y. Hayakawa, H. Honjo, and Y. Sawada, Phys. Rev. Lett. **53**, 286 (1984).

[5] J.S. Langer, Rev. Mod. Phys. **52**, 1 (1980); H. Honjo, S. Ohta, and M. Matsushita, J. Phys. Soc. Jpn. **55**, 2487 (1986).

[6] K.J. Lee, W.D. McCormick, Q. Puyang, and H.L. Swinney, Science **261**, 189 (1993).

[7] T. Vicsek, M. Cserzo, and V.K. Horváth, Physica A **167**, 315 (1990).

[8] P.G. Saffman and G.I. Taylor, Proc. R. Soc. London, Ser. A **245**, 312 (1958).

[9] D.A. Kessler and H. Levine, Adv. Phys. **37**, 255 (1988), and references therein.

[10] P.G. Saffman, Q. J. Mech. Appl. Math. **12**, 146 (1959); S.D. Howison, J. Fluid Mech. **167**, 439 (1986); D. Bensimon and P. Pelcé, Phys. Rev. A **33**, R4477 (1986).

[11] M. Mineev-Weinstein, Physica D **43**, 288 (1990).

[12] D. Bensimon, L.P. Kadanoff, S. Liang, B.I. Shraiman, and C. Tang, Rev. Mod. Phys. **58**, 977 (1986).

[13] W-S. Dai, L.P. Kadanoff, and S.-M. Zhou, Phys. Rev. A **43**, 6672 (1991).
[14] M. Mineev-Weinstein and S.P. Dawson, Phys. Rev. E **50**, R24 (1994).
[15] S.P. Dawson and M. Mineev-Weinstein, Physica **73**, 373 (1994).
[16] M. Siegel and S. Tanveer, Phys. Rev. Lett. **76**, 419 (1996); M. Siegel, S. Tanveer, and W-S. Dai, J. Fluid Mech. **323**, 201 (1996).
[17] M. Mineev-Weinstein, Phys. Rev. Lett. (to be published).
[18] L. Paterson, J. Fluid Mech. **113**, 513 (1981).
[19] M.J. Ablowitz and H. Seguar, *Solitons and the Inverse Scattering Transform* (SIAM, Philadelphia, 1981).
[20] N. Ercolani, M.G. Forest, D.W. McLaughlin, and A. Sinha, J. Nonlinear Sci. **3**, 393 (1993).
[21] P.Ya. Polubarinova-Kochina, Dokl. Akad. Nauk SSSR **47**, 254 (1945) [C. R.(Dokl.) Acad. Sci. **47**, 250 (1945)]; L.A. Galin, Dokl. Akad. Nauk SSSR **47**, 246 (1945) [C. R. (Dokl.) Acad. Sci. **47**, 246 (1945)].
[22] S. Richardson, J. Fluid Mech. **56**, 609 (1972).
[23] M. Mineev-Weinstein, Phys. Rev. E **47**, R2241 (1993).
[24] M. Mineev-Weinstein (unpublished).
[25] H. Tomé *et al.*, Phys. Fluids A **1**, 224 (1989).
[26] See, e.g., I.S. Gradshtein and I.M. Ryzhik, *Table of Integrals, Series and Products* (Academic Press, New York, 1980), p. 1120.
[27] C. Foias, B. Nicolaekno, G. R. Sell, and R. Temam, J. Math. Pures Appl. **67**, 197 (1988); R. Temam, *Infinite Dimensional Dynamical Systems in Mechanics and Physics* (Springer-Verlag, New York, 1988); M.S. Jolly, I.G. Kevrekidis, and E.S. Titi, Physica D **44**, 38 (1990); N. Aubry, P. Holmes, J.L. Lumley, and E. Stone, J. Fluid Mech. **192**, 115 (1988).
[28] O. Thual, U. Frisch, and M. Hénon, J. Phys. (France) **46**, 1485 (1985); O. Kupervasser, Z. Olami, and I. Procaccia, Phys. Rev. Lett. **76**, 146 (1996); Z. Olami, B. Galanti, O. Kupervasser, and I. Procaccia, Phys. Rev. E **67**, 2649 (1997).